LIMNOLOGY
and
OCEANOGRAPHY

ASLO

Limnol. Oceanogr. 65, 2020, 2261–2277

doi: 10.1002/lno.11451

Near streambed flow shapes microbial guilds within and across trophic levels in fluvial biofilms

Ute Risse-Buhl,[1*] **Christine Anlanger**,[1,2] **Antonis Chatzinotas**,[3,4,5] **Christian Noss**,[2,6] **Andreas Lorke**,[2] **Markus Weitere**[1]

[1]Department of River Ecology, Helmholtz Centre for Environmental Research – UFZ, Magdeburg, Germany
[2]Institute for Environmental Sciences, University of Koblenz-Landau, Landau, Germany
[3]Department of Environmental Microbiology, Helmholtz Centre for Environmental Research – UFZ, Leipzig, Germany
[4]Institute of Biology, Leipzig University, Leipzig, Germany
[5]German Centre for Integrative Biodiversity Research (iDiv) Halle-Jena-Leipzig, Leipzig, Germany
[6]Federal Waterways Engineering and Research Institute, Karlsruhe, Germany

Abstract

Flow is an important physical driver of biofilm communities. Here, we tested the effects of the near bed flows in two mountainous stream reaches on the structure of biofilm microbial guilds (autotrophs, heterotrophic bacteria, and heterotrophic protists) within and across trophic levels. Near bed flow velocity and turbulent kinetic energy were important physical drivers for structuring the communities within and across guilds of the multitrophic fluvial biofilms. The effects of flow were nested in a seasonal and spatial (across-streams) context. Changes in physicochemical factors (temperature, light, dissolved carbon, and nutrients) along the reaches were alike in both streams suggesting that environmental boundary conditions at larger temporal scales were responsible for the seasonal differences of biofilm communities, whereas locally microbial diversity was shaped by near bed flow. Typically, the abundance of autotrophs increased with flow, indicating that biofilms shifted toward increasing autotrophy with increasing shear forces. Filamentous autotrophs seemed to provide protected habitats from the shear forces for smaller sized bacteria. Heterotrophic protist abundance decreased with flow leading to decreasing grazer to prey ratio. Bacteria thus benefitted from a reduction in grazing pressure at faster flowing, more turbulent sites. Our results suggest that near bed flow can impact the magnitude and direction of matter fluxes through the microbial food web and possibly affect ecosystem functioning of fluvial biofilms.

In fluvial ecosystems, the majority of microbes including bacteria, cyanobacteria, and protists live associated to surfaces forming biofilms (hereafter fluvial biofilms) (Lock et al. 1984; Wetzel 2001; Battin et al. 2016). These fluvial biofilms are hotspots of organic matter cycling, ecosystem respiration, and primary production (e.g., Haack and McFeters 1982) and represent the main food source for higher trophic levels such as the meio- and macrofauna (Augspurger et al. 2008; Norf et al. 2009; Majdi et al. 2012). The flow of water interacts with bed roughness resulting in a complex pattern of temporally and spatially variable flows in fluvial ecosystems (Statzner et al. 1988; Hart and Finelly 1999; Biggs et al. 2005; Risse-Buhl et al. 2017). The interaction between flow and the dynamic multitrophic biofilm communities has implications for functioning and performance of fluvial biofilms and, correspondingly, for ecosystem processes (Battin et al. 2003*a*, 2016).

Flow properties of fluvial ecosystems vary on temporal scales ranging from milliseconds to centuries and on spatial scales ranging from bed roughness to catchment. Of particular relevance for biofilm community structure and function is flow variability at temporal scales of milliseconds to minutes and spatial scales of bed roughness to channel width where growth conditions of biofilms are controlled through shear forces and mass-transfer processes at the microscale (Biggs 1996; Biggs et al. 2005; Battin et al. 2007). For example, with increasing near bed turbulence fluvial biofilms are growing more compact, with fewer channels and lower protrusion into the water column, all increasing the resistance toward higher shear forces (Battin et al. 2003*b*; Risse-Buhl et al. 2017). Increasing turbulence reduces the distance over which nutrient exchange is controlled by molecular diffusion, and hence enhances nutrient supply for microbial cells within biofilms

*Correspondence: ute.risse-buhl@ufz.de

Additional Supporting Information may be found in the online version of this article.

(Lorke et al. 2003; Bryant et al. 2010). Effects of turbulence on biofilm architecture and on the abundance of heterotrophic bacteria and autotrophs have been mainly studied under simplified hydrodynamic conditions in artificial systems (e.g., Stoodley et al. 1999; Battin et al. 2003*b*; Teodósio et al. 2010; Graba et al. 2013). In artificial systems, flow variability is expressed by different physical descriptors (Besemer et al. 2009*b*; Singer et al. 2010; Li et al. 2018) including the temporally averaged near bed flow velocity ($\bar{u}$) and turbulent kinetic energy (TKE; accounting for temporal velocity fluctuations). Not one single, but a combination of different physical descriptors of near bed flow predicts biomass, community composition, and function of biofilms under simplified flow conditions in flow cells or flumes (Besemer et al. 2009*b*; Singer et al. 2010; Li et al. 2018; Polst et al. 2018). However, it is still unknown if these predictors for near bed flow of experimental systems explain the variability of biofilm communities matured under temporally and spatially variable flows of fluvial ecosystems.

Microorganisms within environmental biofilms can be roughly classified in trophic-functional guilds, that is, autotrophic cyanobacteria and algae (hereafter autotrophs), heterotrophic bacteria as well as phagotrophic protists (i.e., protists grazing upon other microbes; hereafter heterotrophic protists). Existing studies focused on the interaction between near bed flow and single microbial guilds in epilithic biofilms (e.g., Stevenson 1996; Besemer et al. 2009*b*; Risse-Buhl and Küsel 2009). For example, cyanobacteria and algae can develop filamentous growth and streamers under a range of near bed flows and thereby modulate the flow microenvironment and reducing shear forces on underlying biofilms (Reiter and Carlson 1986; Stevenson 1996; Besemer et al. 2007). These filamentous structures constitute a preferable habitat for bacteria over the biofilm base due to enhanced mass-transfer of nutrients (Besemer et al. 2009*a*). Additionally, the interstitial spaces of filamentous structures are potential refuges for heterotrophic protists (Schönborn 1996*b*). Without such refuges, the abundance and richness of heterotrophic protists is gradually reduced by increasing flow velocities (Schmitz 1985; Primc and Habdija 1987; Risse-Buhl and Küsel 2009). Ciliates lacking specific features to attach or stay associated to surfaces are detached at increasing flow (Risse-Buhl and Küsel 2009), while the microtopography of the surface can offset the effect of flow and affect the spatial distribution of the smaller sized flagellates (Willkomm et al. 2007).

Multitrophic communities within fluvial biofilms are diverse and are characterized by various interactions within the microbial food webs. For instance, primary producers interact with secondary consumers (bacteria), and both are taken up by grazing heterotrophic protists (Weitere et al. 2018). In such multitrophic systems, complex interactions including indirect effects can occur in response to external drivers (Wey et al. 2008). So far, the multitrophic communities of fluvial biofilms as a whole has rarely been assessed (but see Romaní et al. 2014; Ritz et al. 2017; Bengtsson et al. 2018) and hence effects of near bed flow within as well as across microbial guilds are poorly understood. Knowledge on single guilds indicates that near bed flow causes a guild-specific trait dependent shift of microbial communities (growth form of autotrophs, e.g., unicellular vs. filamentous morphotypes, and function, e.g., food preference of heterotrophic protists), resulting in effects on the overall trophic structure of biofilms.

In the present study, we analyzed the role of near bed flow in mountainous streams on three microbial guilds of fluvial biofilms, namely autotrophs, heterotrophic bacteria, and heterotrophic protists. We hypothesize that the abundances, but not the diversity of small-sized heterotrophic bacteria and of autotrophs with specialized holdfast features increases, whereas the abundance of free moving heterotrophic protists decreases with increasing near bed flow. Heterotrophic bacteria and protists will remain unaffected by shear forces at increased near bed flow if filamentous autotrophs shape the fluvial biofilm. Correspondingly, we expect a shift in the across microbial guild and trophic structure toward higher autotrophy (dominance of autotrophs) and lower grazer control with increasing near bed flow.

Materials

Field site characterization

Fluvial biofilms were sampled at free-flowing stream reaches featuring contrasting near bed flow in two coarse grained mountainous streams, namely Kalte Bode (51°44′33″N, 10°42′12″E, 470 m a.s.l.) and Selke (51°41′12″N, 11°15′31″E, 210 m a.s.l.), along stream reaches being, respectively, 588 m and 510 m long. Both streams are located 40 km apart in the Bode catchment (Harz Mountains, Saxony-Anhalt, Germany) belonging to a long-term monitoring area of the Helmholtz Terrestrial Environmental Observatories (TERENO) (Kamjunke et al. 2015*b*; Wollschläger et al. 2017). The mountainous streams are comparable in their bed morphology with pool-riffle sequences. Samples were collected following a correlative design at randomly chosen spots along the study reaches within 5 d. In order to test the generalizability of interactions, the effects of near bed flow on fluvial biofilms were quantified at three seasons, namely April/May 2014 (hereafter Apr 2014), August 2014 (hereafter Aug 2014), and May/June 2015 (hereafter Jun 2015).

Discharge data were provided by the Flood Prediction Centre of the state Saxony-Anhalt (http://www.hochwasservorhersage.sachsen-anhalt.de), which were measured 1.5 km upstream and 2 km downstream of the study reaches of the Kalte Bode and Selke, respectively. The long-term baseflow estimated from the long-term mean lowest discharge (MNQ) and mean discharge (MQ) at the sites of the Kalte Bode estimated 0.18 $m^3 s^{-1}$ and 0.72 $m^3 s^{-1}$ and at the sites of the Selke estimated 0.24 $m^3 s^{-1}$ and 1.52 $m^3 s^{-1}$, respectively. Over both streams, discharge during and well before (> 3 weeks) samplings in Apr 2014 and Jun 2015 was in the range of MNQ and MQ (Fig. 1, Supporting Information Table S1). In Aug

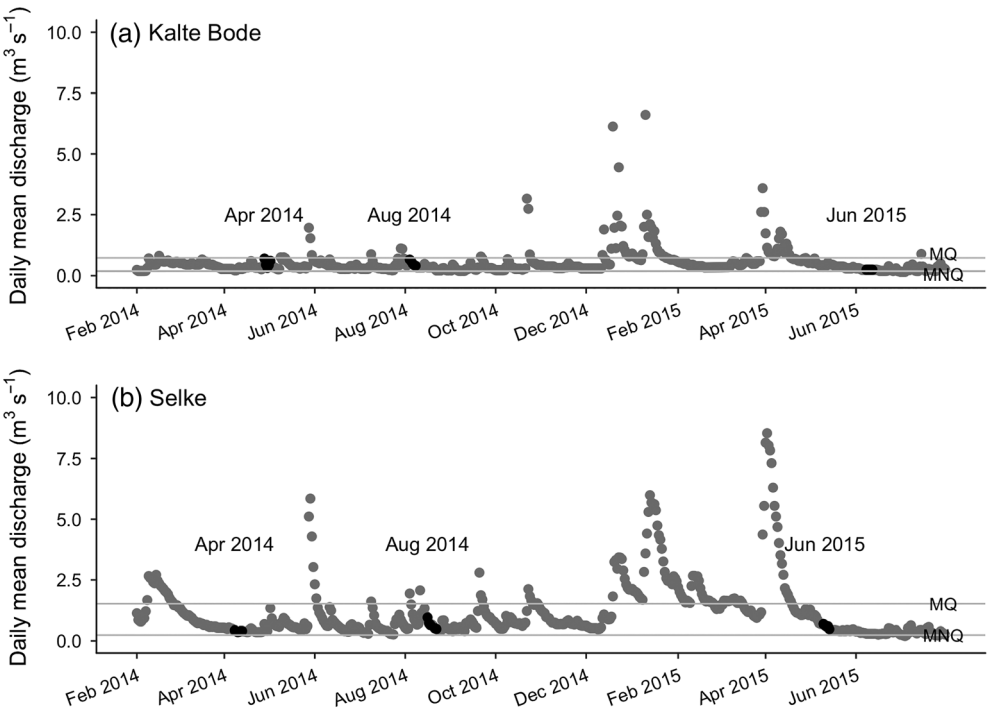

Fig. 1. Changes in daily mean discharge ($m^3\ s^{-1}$) of (**a**) Kalte Bode and (**b**) Selke from February 2014 to July 2015. Discharge during samplings is indicated by black dots. Solid gray lines indicate characteristic hydrologic descriptors, namely long-term mean lowest discharge (MNQ, lower line) and mean discharge (MQ, upper line).

2014, discharge of both streams was slightly higher than MNQ for 2 d 1 week before the samplings. Bankfull discharge was never observed indicating that there was no bed forming discharge event during and between the sampling periods (Fig. 1).

Five light loggers (HOBO Pendant Temperature/Light Data Logger UA-002-64, Onset Computer Corporation, Bourne, MA, U.S.A.) were deployed along the stream reaches to characterize the sum of photosynthetic active radiation (PAR) during the 5-d samplings. Water temperature (T), oxygen concentration (O_2), pH, and conductivity were logged at 15 min interval using an EXO2 multiparameter probe (YSI, Yellow Springs, OH, U.S.A.). Filtered water samples were analyzed for dissolved organic carbon (DOC; pore size 0.45 μm), dissolved inorganic nitrogen (DIN; pore size 0.2 μm) comprising nitrate (NO_3-N), nitrite (NO_2-N) and ammonium (NH_4-N), and soluble reactive phosphorous (SRP; pore size 0.2 μm), and unfiltered water samples for chlorophyll *a* (collected on GF/F) (*see* Risse-Buhl et al. 2017 for description of methods). Over both streams, photosynthetic active radiation (PAR.sum, given as 5-d sum of the stream reach mean) was lowest due to the dense canopy cover of the riparian vegetation and T was highest in Aug 2014. DOC concentrations were comparable between streams (Supporting Information Table S2). In contrast, DIN and SRP were always higher in stream water of the Selke compared to that of the Kalte Bode resulting in a lower DIN to SRP ratio (DIN : SRP) in the latter. Hence, the Kalte Bode was poorer and the Selke richer in nutrients (*see* Risse-Buhl et al. 2017).

Measurement and analysis of the near bed flow

The sampling spots in both streams were characterized by grains with sizes ranging from medium-sized gravel to boulders, being between 1–32 cm long and 0.5–27 cm wide. Water depth of sampled biofilms ranged between 9 and 50 cm. At each sampling spot, time series of the three-dimensional near bed flow velocity were measured with a multistatic acoustic Doppler velocity (ADV) profiler (Vectrino II, Nortek AS, Norway) at 64 Hz for 20 min. We only processed data of the Vectrino so-called sweet spot, which was 2.3 cm above the stream bed (*see* Koca et al. 2017; Risse-Buhl et al. 2017).

From filtered velocity time series, we performed a coordinate rotation, forcing mean values of the vertical and transversal velocity component to zero to account for misalignments of the probe head. Measurements noise was removed from the velocity components by low-pass filtering while the cutoff frequency of the filter was estimated from power spectra of each velocity time series and each velocity component. Noise was identified in the spectra as the breakpoint in spectral slope where the spectra flattened at high frequencies. We calculated the mean flow velocity ($\bar{u}$) as the magnitude of the Reynolds averaged mean flow velocity according to

Table 1. Minimum and maximum range of near bed mean flow velocity ($\bar{u}$) and TKE at the two streams and three seasons studied.

Stream	Sampling date	Season	No. of samples	$\bar{u}$ (m s^{-1})	TKE (m^2 s^{-2})
Kalte Bode	28th Apr–2nd May 2014	Apr 14	27	0.064–0.410	8.16×10^{-4} to 1.33×10^{-2}
	4th–7th Aug 2014	Aug 14	26	0.035–0.450	3.91×10^{-4} to 1.30×10^{-2}
	8th–11th Jun 2015	Jun 15	25	0.026–0.343	4.10×10^{-4} to 4.28×10^{-2}
Selke	8th–13th Apr 2014	Apr 14	12	0.025–0.506	9.31×10^{-4} to 9.49×10^{-2}
	17th–22nd Aug 2014	Aug 14	17	0.032–0.725	10.19×10^{-4} to 4.65×10^{-2}
	11th–14th May 2015	Jun 15	31	0.031–0.768	13.26×10^{-4} to 2.97×10^{-2}

$$\bar{u} = \frac{1}{N}\sum_{i=1}^{N} u_i$$

where $\bar{u}$ and N denote the longitudinal component of the velocity vector and the number of measurements at each location, respectively. TKE was estimated from the variance of filtered velocity components (u, v, w) as

$$\mathrm{TKE} = \frac{1}{2}\left(\overline{u'^2} + \overline{v'^2} + \overline{w'^2}\right)$$

where the prime denotes deviations of instantaneous velocities from their mean value.

Handling and analysis of biofilm samples

Following the hydrodynamic measurement, a macrophotograph of each stone was taken where a laser pointer highlighted the precise location of the Vectrino sampling spot before carefully removing the stone from streambed. The biofilm covering this location was mechanically removed by brushing the stone's surface twice with a clean tooth brush and suspended in 30 mL sterile filtered stream water (pore size 0.2 μm). Rinsing the stones surface presumably resulted in the collection of some loosely associated and mobile cells adjacent to the location of the Vectrino sampling spot. The applied sampling procedure allowed a correlation between biofilm characteristics and physical descriptors.

The area covered by the removed biofilm was projected to a tinfoil. The area of each tinfoil piece was quantified with the software Fiji (Schindelin et al. 2012). The biofilm suspension was homogenized by ultrasonic treatment (Bandelin Sonorex RK52, Berlin, Germany) for 2 min and subsamples were prepared for microscopic observations and molecular analyses.

Microscopically, we quantified bacteria and analyzed abundance, diversity, and community structure of autotrophs and heterotrophic protists (number of samples are provided in Table 1, Supporting Information Tables S3, S4). Bacteria in a subsample of 0.1–0.5 mL (fixed with formaldehyde, 3.7% final concentration) were filtered onto black polycarbonate membranes (pore size 0.2 μm), stained with acridine orange and counted using an epifluorescence microscope at ×1000 magnification (Axioskop2, Zeiss, Jena, Germany) (Kamjunke et al. 2015*a*). For the quantification of autotrophs, a subsample of 0.5–3 mL (fixed with formaldehyde, 3.7% final concentration) was placed in an Utermoehl chamber. Cells were allowed to settle overnight and were observed at ×400 magnification using phase contrast of an inverted light microscope (Observer Z1, Zeiss, Jena, Germany). Cyanobacteria and green algae were grouped according to their cell morphology traits in coccoid, comma-like, colonial (e.g., genera *Pediastrum* and *Scenedesmus*) and filamentous morphotypes. Diatoms were identified to the level of genera (Cox 1997) and grouped according to their cell morphology traits in centric (mainly filamentous colonies of *Melosira*) and pennate morphotypes.

Heterotrophic protists were observed alive using a light microscope (Lab A1, Zeiss, Jena, Germany) within 24 h after sampling. Ciliates and testate amoeba were scanned in 0.2–2 mL sample volume placed in a Sedgewick Rafter chamber (calibrated for 1 mL, one to two subsamples) at ×100 magnification. Four subsamples of 15 μL were placed on a glass slide, covered by a cover slip (15 × 15 mm) and five lines each were scanned for flagellates and naked amoeba at ×400 magnification. Heterotrophic protists were identified to the lowest possible taxonomic level; ciliates and testate amoeba were identified to the genus or species level (Page and Siemensma 1991; Foissner and Berger 1996; Patterson 2003), flagellates to class or family level (Jeuck and Arndt 2013) and naked amoeba were grouped according to their morphotype (Smirnov and Goodkov 1999). According to the functional trait of utilized food source, heterotrophic protists were grouped in bacterivorous (mainly feeding on bacteria), bacteri-algivorous (feeding on bacteria and autotrophs), omnivorous (feeding on bacteria and all kinds of protists), and predators (feeding exclusively on other heterotrophic protists) (Foissner and Berger 1996).

General shifts in bacterial and micro-eukaryotic diversity and community composition were further analyzed using 16S (representing all bacteria) and 18S (representing autotrophic and heterotrophic eukaryotic microbes) rRNA gene-based terminal restriction fragment length polymorphism (T-RFLP), respectively. DNA was extracted using NucleoSpin™ Tissue kit (Macherey-Nagel) and stored at −20°C. Polymerase chain reaction (PCR) was performed using MyTaq™ Mix (Bioline, Luckenwalde, Germany) and 5 pmol of each primer. For 16S rRNA gene-based T-RFLP, fluorescein amidite (FAM) labeled bacteria-specific forward primer UniBac27f (Lane 1991) and reverse universal primer Univ519r

(Lane et al. 1985) were used; for 18S rRNA gene-based T-RFLP, FAM-labeled eukaryote specific primers Euk20f and Euk516r (Amann et al. 1990; Euringer and Lueders 2008) were used. Thermocycling for 16S rRNA genes was carried out with an initial denaturation at 95°C (5 min), followed by 30 cycles of denaturation at 95°C (1 min), annealing at 56°C (1 min) and elongation 72°C (1 min), a 10 min extension step at 72°C. PCR conditions for 18S rRNA gene amplification consisted of initial denaturation for 3 min at 95°C and cycles of denaturation for 15 s at 95°C, annealing for 15 s at 58°C and elongation for 10 s at 72°C followed by final elongation of 10 min at 72°C. Fluorescently labeled PCR products were purified using SureClean (Bioline, Luckenwalde, Germany) and quantified by gel quantification (Kuppardt et al. 2018). Cleaned products were then subjected to overnight digestion with the restriction enzyme *Msp*I (NEB, Ipswich, MA, U.S.A.) for 16S rRNA genes and *Bst*UI (NEB) for 18S rRNA genes (Euringer and Lueders 2008; Glaser et al. 2015), respectively. Each digestion reaction contained 20 ng of DNA, 2 U of restriction enzyme and 1 μL of CutSmart® Buffer (NEB) in a final reaction volume of 10 μL. After digestion, reactions were purified and fluorescently labeled terminal restriction fragments (T-RFs) from 50 to 500 bp analyzed as described in Glaser et al. (2015) and Kuppardt et al. (2018) in an ABI Prism® 3130 genetic analyser (Applied Biosystems, Foster City, CA, U.S.A.) using the GeneMapper software (Applied Biosystems). After normalization, the relative abundance of each T-RF was calculated as the percentage of the combined peak area of each sample. We are aware that sequence-based approaches provide deeper insight into the single components of the bacterial and micro-eukaryotic community (Grossmann et al. 2016). Still, fingerprinting methods, such as T-RFLP, are useful to observe shifts in communities under different treatments (Glaser et al. 2014, 2015; Kuppardt et al. 2018) and the general trends are comparable with the results of sequencing based approaches (van Dorst et al. 2014; Santillan et al. 2019).

Data handling and statistical analyses

All statistical analyses were performed in R (version 3.4.3/2017; R Development Core Team 2018) using the RStudio console (version 1.1.383). For graphics art, we used the R package "ggplot2" (version 2.2.1.) Before statistical analyses, cell count data were transformed $\log_{10}(x + 1)$ and hydrodynamic data $\log_{10}(x)$, whereas relative abundances of prokaryotic 16S rRNA gene T-RFs and micro-eukaryotic 18S rRNA gene T-RFs, multitrophic metrices and diversity indices were not transformed.

Abundance of microbial guilds was expressed as cells cm^{-2} epilithic area. Relative abundance of 16S and 18S rRNA gene T-RFs (as an approximate indication for dominant members of the communities) and morphotype specific abundance were used to perform indicator species analysis (function "multipatt" of the package "indicspecies"; De Caceres and Legendre 2009) and to calculate diversity indices (function "diversity" of the R package "vegan"). The simplest index used to represent diversity was richness, which is the number of T-RFs or morphotypes present in one sample (Whittaker 1972). To combine measures of richness and abundance, we employed the diversity indices of the Hill family, namely Shannon-Weaver, Simpson, and Inverse Simpson indices, which decrease in their sensitivity toward rare species (Hill 1973). We display results for Shannon-Weaver diversity index in the manuscript, since trends shaped by near bed flow were comparable among all diversity measures. Pielou's evenness displays to which degree individuals are split among T-RFs or morphotypes. With decreasing evenness, a decreasing number of T-RFs or morphotypes dominate the community.

Abundance data were used to calculate multitrophic metrices such as ratios of bacteria/autotrophs, bacteria/flagellates, bacteria/ciliates, and autotrophs/ciliates (e.g., Berninger et al. 1991). To compare morphological traits of autotrophs, their biovolume was calculated using length, width, and depth measurements of up to 30 cells and most similar geometric forms (Hillebrand et al. 1999). To detect changes in the abundances of the three microbial guilds, the relative biovolume contribution of morphological traits of autotrophs and the relative abundance of functional traits of heterotrophic protists, all samples were grouped in two classes of TKE either lower or higher than the mean $\log_{10}$ transformed TKE of all samples of −2.5, corresponding to $3.16 \times 10^{-3}\ m^2\ s^{-2}$.

Pearson product momentum correlation coefficients (function "cor.test") were computed for interactions between hydrodynamic measures. To test if near bed flow significantly affected changes in biofilm guilds (abundance, diversity, and multitrophic metrices) and for stream and season effects, a two-factorial analysis of covariance (ANCOVA, function "aov") with stream and season as factors and either $\bar{u}$ or TKE as covariate was performed. Outliers within each data set of season and stream were removed according to mean ± 3SD. Spearman rank correlation (function "cor.test") was used to test the effect of near bed flow on biofilm guilds stream- and season-wise.

In order to identify environmental factors that significantly contribute to the variability in community structure of biofilm guilds, we used distance-based redundancy analysis (db-RDA; function "capscale" of the R package "vegan") with the Bray-Curtis dissimilarity measure (McArdle and Anderson 2001). T-RFs and morphotypes that occurred in less than three samples were removed prior to the analyses. Centered and standardized environmental variables as $\log_{10}$ transformed near bed flow ($\bar{u}$ and TKE) and untransformed physicochemistry (T, DOC, DIN : SRP and PAR.sum) had an acceptable level of multicollinearity as indicated by variance inflation factors of less than 3 and therefore uniquely contributed to the ordination (Oksanen et al. 2017). The significantly explaining variables that were revealed by stepwise forward and backward selection (function "step" and "ordistep") were included in the ordination of the reduced models.

Results

Near bed flow

The mean flow velocity ($\bar{u}$) at both sampling sites (Kalte Bode and Selke) and all three seasons (Apr 2014, Aug 2014,

Table 2. Results of two independent two-factorial ANCOVA for each measure of near bed flow with stream and season as factors and mean flow velocity ($\bar{u}$) and TKE as covariate.

	$\bar{u}$							TKE							
df	Stream 1	Season 2	$\bar{u}$ 1	Stream × Season 2	Stream × $\bar{u}$ 1	Season × $\bar{u}$ 2	Stream × Season × $\bar{u}$ 2	Stream 1	Season 2	TKE 1	Stream × Season 2	Stream × TKE 1	Season × TKE 2	Stream × Season × TKE 2	df residuals
Abundance															
Heterotrophic bacteria total	-	***	-	-	-	-	-	-	***	-	-	-	-	-	125
Autotrophs total	-	***	-	-	-	-	-	-	***	-	-	-	-	-	38
Cyanobacteria	-	***	-	-	-	-	-	-	***	*	-	-	-	-	38
Diatoms	-	***	**	-	-	-	-	-	***	**	*	*	-	-	38
Green algae	-	-	-	-	-	-	-	-	***	**	*	*	-	-	38
Heterotrophic protists total	-	***	-	**	-	-	-	-	***	-	**	-	*	-	122
Flagellates	-	***	*	*	**	-	-	-	***	*	*	-	*	-	122
Naked amoeba	-	***	-	-	-	-	-	-	***	-	-	-	-	-	122
Testate amoeba	-	**	**	-	-	-	-	-	**	**	-	-	*	-	122
Ciliates	***	***	**	-	**	*	-	***	***	**	-	**	**	-	122
Diversity indices															
Bacteria 16S T-RFs															
Richness	-	*	-	-	-	-	-	-	**	-	-	-	**	-	74
Shannon	*	*	-	-	-	-	-	*	*	-	-	-	**	-	72
Pielous evenness	**	**	-	-	-	-	-	**	**	-	-	-	*	-	74
Micro-eukaryotes 18S T-RFs															
Richness	-	*	*	-	-	-	-	-	**	***	-	-	-	-	75
Shannon	-	-	*	-	-	-	-	-	-	**	-	-	-	*	75
Pielous evenness	-	-	-	-	-	-	-	-	-	-	-	-	*	*	75
Autotrophs															
Richness	-	***	**	**	-	-	-	-	***	**	***	-	-	-	38
Shannon	-	***	-	-	-	-	*	-	***	*	-	-	**	-	38
Pielous evenness	-	-	-	*	-	-	-	-	-	-	*	-	*	-	38
Heterotrophic protists															
Richness	-	***	***	*	-	-	-	-	***	***	*	-	*	-	106
Shannon	-	-	***	***	-	-	-	-	-	***	***	-	-	-	106
Pielous evenness	-	**	**	**	*	-	-	-	**	-	**	-	*	-	106
Multitrophic metrices															
Autotrophs/ bacteria	-	-	-	-	-	-	-	-	-	-	-	-	-	-	37
Flagellates/ bacteria	*	*	**	-	-	-	-	*	*	**	-	-	-	-	83
Ciliates/bacteria	***	-	-	**	*	-	*	***	-	-	***	**	-	-	103
Ciliates/ autotrophs	*	**	-	-	-	-	-	-	**	-	-	-	-	-	28

***$p < 0.001$, **$p < 0.01$, *$p < 0.5$, $^{-}p > 0.5$.

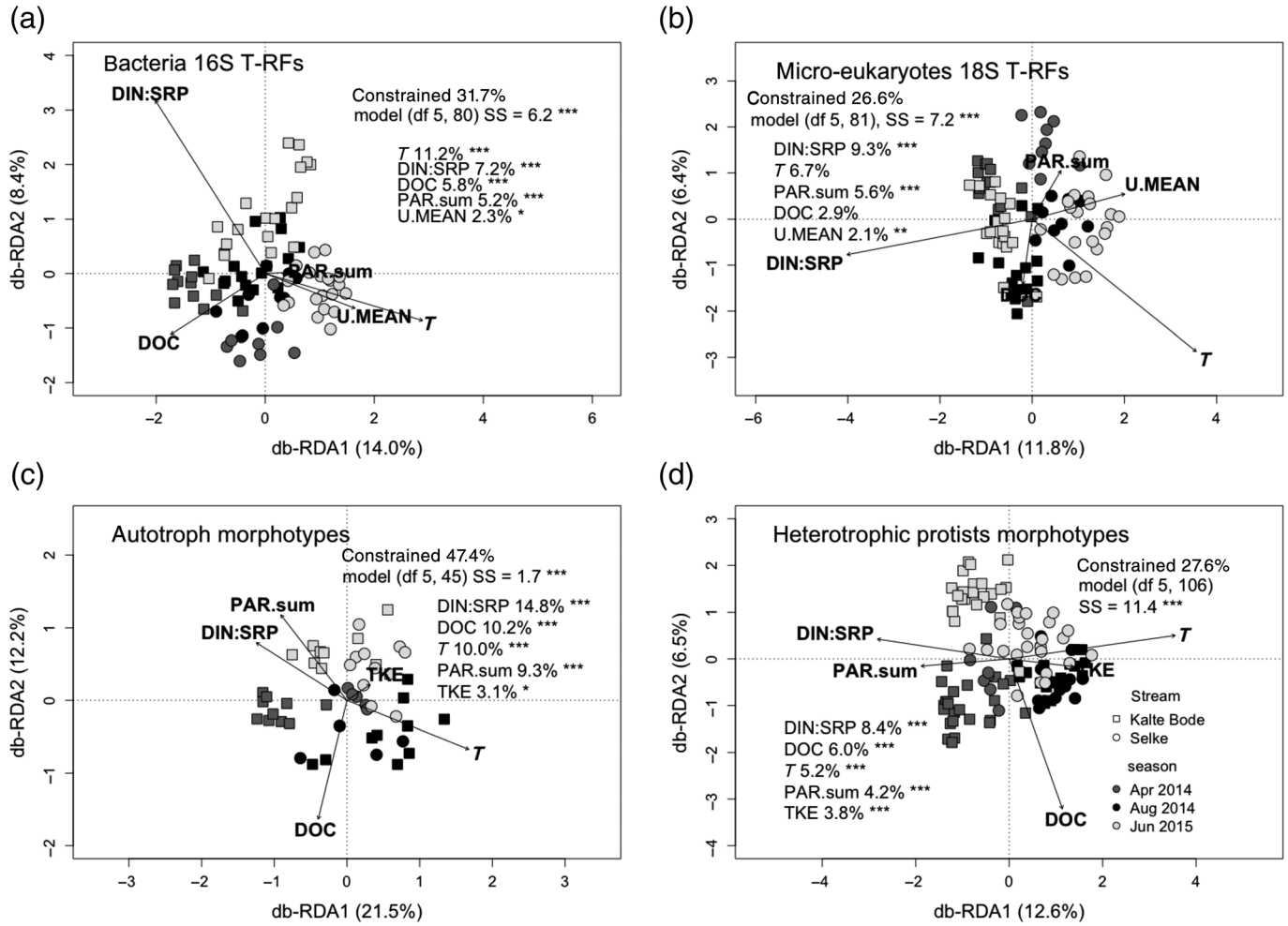

Fig. 2. db-RDA of the community structure of (**a**) bacteria (based on 16S rRNA gene T-RF profiles), (**b**) micro-eukaryotes (based on 18S rRNA gene T-RF profiles), (**c**) autotroph morphotypes, including cyanobacteria and eukaryotic algae, and (**d**) heterotrophic protists morphotypes, including flagellates, amoeba, and ciliates. Abundance data were $\log_{10}(x+1)$ transformed and environmental factors were centered and standardized. Environmental factors as mean flow velocity (U.MEAN), TKE, temperature (*T*), DOC, 5-d sum of photosynthetic active radiation (PAR.sum), ratio of DIN to SRP were selected by forward and backward selection, and exclusively significant contributing factors are displayed. ANOVA was used to test for the goodness of the reduced model and to calculate the contribution of environmental factors to explain the variability in the data set. Significance levels: ***$p < 0.001$, **$p < 0.01$, *$p < 0.05$.

and Jun15) varied over one-order of magnitude, ranging from 0.025 to 0.768 m s^{-1} (Table 1). TKE ranged from 3.91×10^{-4} to 9.49×10^{-2} m^2 s^{-2}, spanning two-orders of magnitude (Table 1). Over all streams and seasons, TKE and $\bar{u}$ were positively correlated ($R^2 = 0.69$, $p < 0.001$).

Effects of flow on microbial guilds in spatial-seasonal context

The effects of flow were nested in a spatial (across-streams) and seasonal context. Regarding the flow effect, both the two-factorial ANCOVA and the db-RDA analyses revealed that $\bar{u}$ and TKE were important for structuring the communities within guilds of the multitrophic fluvial biofilms (Table 2, Fig. 2). Guild-specific and group-specific abundance and diversity of autotrophs and heterotrophic protists but not bacteria were significantly ($p < 0.05$) affected by $\bar{u}$ and TKE (Table 2). Either $\bar{u}$ or TKE were chosen by permutation procedure possibly due to the positive correlation of both variables (see above). Either $\bar{u}$ or TKE significantly explained between 2.3% and 3.8% of the variability in community structure of all microbial guilds (Fig. 2).

Moreover, the two-factorial ANCOVA revealed that in the majority of cases the abundance and diversity of microbial guilds varied with season rather than with stream (Table 2). Seasonally varying physicochemical factors such as *T*, DOC, and PAR.sum (Supporting Information Tables S1, S2) significantly explained between 2.6% and 10.2% of the variability in the community structure of microbial guilds (Fig. 2). DIN : SRP varying seasonally and between streams explained 7.2–14.8% of the variability in the community structure of microbial guilds (Fig. 2).

We separated the data sets and visualized the correlations (Spearman ρ) that tested the effect of near bed flow on guild- and group-specific abundance and diversity for each stream and season (Fig. 3). In detail, bacterial abundance ranging (min–max) from 2.82×10^6 to 1.06×10^9 cells cm^{-2} correlated weakly and was thus not affected by near bed flow (Figs. 3, 4). The abundance of autotrophs ranged between 3.21×10^3 and 5.18×10^4 cells cm^{-2} (guild-specific abundances in Supporting Information Table S3). At the nutrient richer Selke, total and group-specific abundance of autotrophs correlated positively with $\bar{u}$ and TKE except in Apr 2014. At the nutrient poorer Kalte Bode, the abundance of cyanobacteria increased with TKE, whereas the abundance of diatoms and green algae decreased with TKE. Abundance of heterotrophic protists reaching up to 3.63×10^4 cells cm^{-2} decreased in 5 and 4 of 6 samplings with increasing $\bar{u}$ and TKE, respectively. Indicated by the significant interaction of season × $\bar{u}$ and season × TKE (Table 2), the abundances of flagellates, testate amoeba, and ciliates (*see* Supporting Information Table S4) decreased with increasing $\bar{u}$ and TKE in Apr 2014 and Jun 2015 (Fig. 3).

Regarding the diversity of microbial guilds, we observed 77 (50 occurred in more than three samples) bacterial T-RFs (Supporting Information Fig. S1a), 56 (37) micro-eukaryotic T-RFs (Supporting Information Fig. S1b), 29 (23) autotroph morphotypes (list of morphotypes; Supporting Information Table S5), and 185 (67) heterotrophic protist morphotypes (list of morphotypes; Supporting Information Table S6) over all streams and seasons. The identical trends of the Shannon, Simpson, and Inverse Simpson indices suggest that dominant T-RFs and morphotypes were sufficient to explain most of the observed diversity patterns. Over all seasons, the indicator species analyses revealed that bacterial (based on T-RFs) and autotroph (based on morphotypes) community composition was not significantly ($p > 0.05$) different between TKE classes. In contrast, the micro-eukaryotic (based on T-RFs) and heterotrophic protist (based on morphotypes) community at higher TKE was a subset of the community present at lower TKE with,

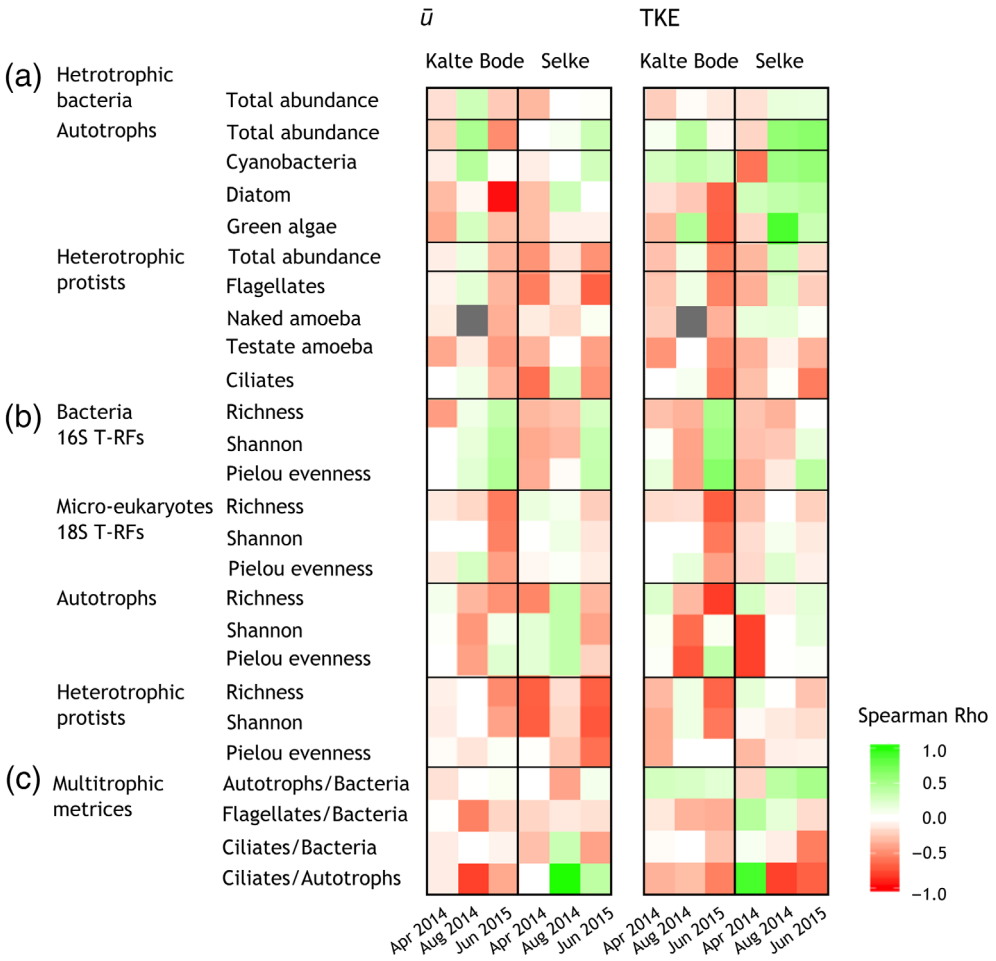

Fig. 3. Heat maps displaying Spearman's Rho of correlations between near bed flow and (**a**) abundances, (**b**) diversity indices and (**c**) multitrophic metrices of microbial guilds in biofilms of the two streams and three seasons studied. Near bed flow is represented by mean flow velocity ($\bar{u}$) and TKE. Abundances of the microbial community (cells cm^{-2}) were $\log_{10}(x + 1)$ transformed.

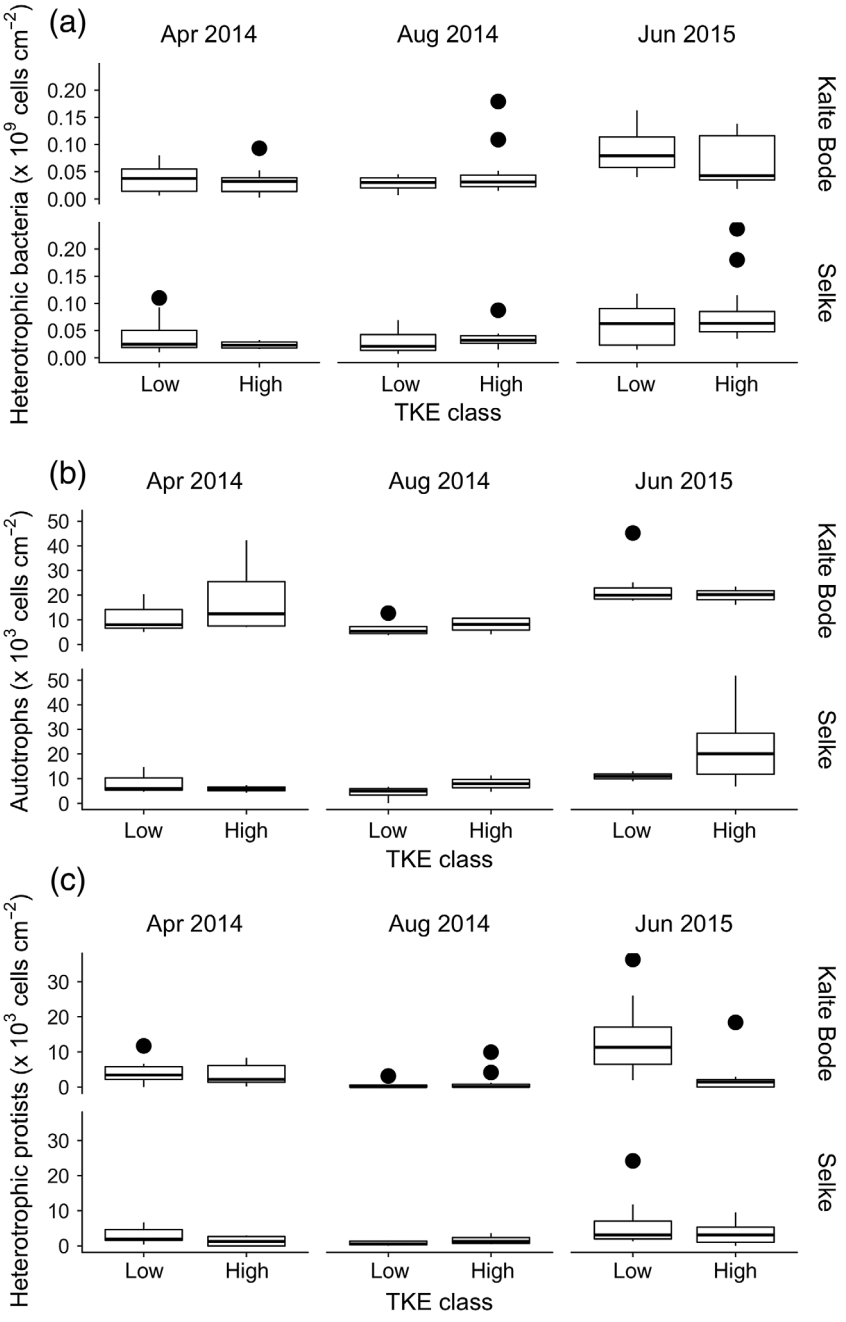

Fig. 4. Abundance of (**a**) bacteria, (**b**) autotrophs, including cyanobacteria and eukaryotic algae, and (**c**) heterotrophic protists, including flagellates, amoeba, and ciliates at two contrasting TKE classes of the two streams and three seasons studied. Low and high TKE classes were separated by the mean TKE of all measurements: $\log_{10}(3.16 \times 10^{-3}\ m^2\ s^{-2}) = -2.5\ m^2\ s^{-2}$. Boxes display 25th and 75th percentile with median indicated as horizontal line, 99th percentile is indicated by vertical lines, and outliers are represented by black dots.

respectively, three T-RFs and nine morphotypes occurring exclusively at lower TKE.

Effects of near bed flow on diversity of the microbial guilds differed between streams and seasons. To identify trends, we focused on significant correlations ($p < 0.05$). Autotroph diversity decreased with increasing $\bar{u}$ and TKE in biofilms of the Kalte Bode, but increased with $\bar{u}$ in biofilms of the Selke in Aug 2014 when light conditions were limiting. Additional negative correlations between autotroph diversity and TKE were observed in the Kalte Bode in Jun 2015 and in the Selke in Apr 2014. In both streams, the overall diversity of bacterial T-RFs increased with $\bar{u}$ and TKE in Jun 2015 whereas it decreased with $\bar{u}$ and TKE in Apr and Aug 2014. In contrast, micro-eukaryotic T-RFLP profiles showed the opposite trend

with increasing $\bar{u}$ and TKE in Jun 2015. Irrespective of season, the morphotype diversity of heterotrophic protists decreased with increasing $\bar{u}$ and TKE.

Effect of flow on trait-specific shifts of microbial guilds

Considering the morphological traits of autotrophs in fluvial biofilms, we observed a larger share of filamentous green algae and a comparable or lower share of single celled diatoms at high TKE compared to low TKE (Fig. 5a). The relative biovolume of filamentous green algae was 1.4× to 16.1× higher at high TKE, except at the Selke in spring (Apr 2014 and Jun 2015) where filamentous green algae were exclusively detected at sites with low TKE. Cyanobacteria biovolume showed contrasting trends between the two streams (Fig. 5a). Similar to green algae, filamentous cyanobacteria had a 1.8× to 6.2× higher relative biovolume at high TKE at the nutrient richer Selke. In contrast, filamentous cyanobacteria had a 1.4× to 2.3× lower relative biovolume at high TKE at the nutrient poorer Kalte Bode. In Apr 2014, filaments of the centric diatom *Melosira* contributed with a mean of 60.4% and 53.4% to the biovolume of the autotroph community in fluvial biofilms at the two contrasting TKE classes of the nutrient poorer Kalte Bode. The relative biovolume of pennate diatoms in this stream was 1.3× to 5.0× lower at high TKE. In contrast, pennate diatoms at the nutrient richer Selke had a 1.3× higher relative biovolume at high TKE. Over both streams, *Navicula* and *Nitzschia* had higher relative biovolume, whereas *Cocconeis* and *Achnanthes* had a lower relative biovolume at high TKE.

Fig. 5. Community composition using (**a**) morphological traits of autotrophs and (**b**) functional traits according to food type used of the heterotrophic protists community at two contrasting TKE classes of the two streams and three seasons studied. Low and high TKE classes were separated by the mean TKE of all measurements: $\log_{10}(3.16 \times 10^{-3}\ m^2\ s^{-2}) = -2.5\ m^2\ s^{-2}$. Cyano, cyanobacteria; Green, green algae.

The relative abundance of the 15 most abundant bacterial T-RFs was comparable between the contrasting TKE classes although seasonal differences were apparent as was observed for autotroph morphotypes (Supporting Information Fig. S1a).

Bacterial abundance was significantly correlated with filamentous autotrophs (two-factorial ANCOVA: $F_{1,38}$ = 6.91, p = 0.012) and more specifically with filamentous cyanobacteria ($F_{1,38}$ = 17.34, $p < 0.001$). Both abundance of bacteria and filamentous autotrophs were positively correlated except in Apr 2014 (Fig. 6).

Interestingly, although total abundances of heterotrophic protists were affected by near bed flow, the relative abundance of heterotrophic protists with distinct feeding preferences did not differ between high and low TKE (Fig. 5b). Bacterivores made up the largest fraction of 15–70% of the total heterotrophic protist abundance in fluvial biofilms. Omnivores and bacterialgivores made up 25-59% and 2-50% of the total heterotrophic protist abundance, respectively. Predators made up the smallest fraction with up to 3% of the total heterotrophic protist abundance. The presence and equal distribution of functional traits of heterotrophic protists indicated multitrophic food web interactions within the fluvial biofilms irrespective of TKE.

Shifts in trophic structure of fluvial biofilms caused by flow

Autotrophy of fluvial biofilms was estimated by means of the ratio of autotrophs to bacteria. The ratio tended to increase with increasing TKE (Fig. 3), indicating that fluvial biofilms shifted toward autotrophy with increasing near bed turbulence.

As measure of trophic structure, we used ratios of grazers to their preferred food (bacteria and autotrophs) indicating grazing pressure and flux of matter within the biofilm food web. All calculated ratios, that is, flagellates to bacteria (significant effect, see Table 2), ciliates to bacteria, and ciliates to autotrophs decreased with increasing near bed flow, except for few cases of positive correlations (Fig. 3). This result indicates a shift in the trophic structure of fluvial biofilms toward a decreasing importance of grazer control with increasing near bed turbulence.

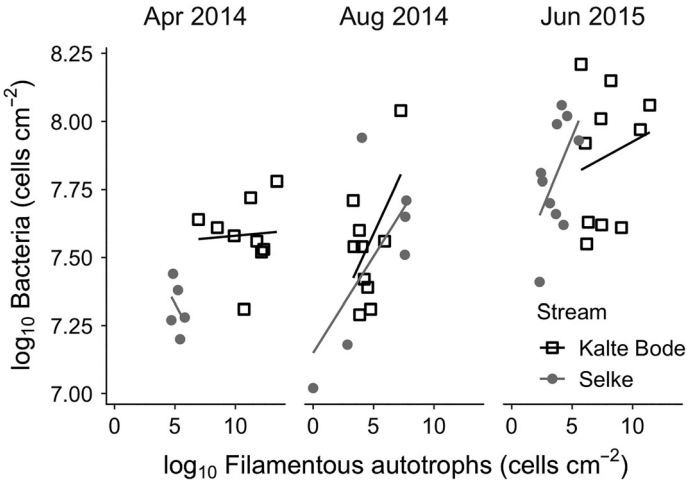

Fig. 6. Correlation between the abundance of filamentous autotrophs (including cyanobacteria, green algae, and the colonies of the centric diatom *Melosira*) and bacteria at the two streams and three seasons studied. Abundance data were $\log_{10}(x + 1)$ transformed.

Discussion

Near bed $\bar{u}$ and TKE as physical drivers for fluvial biofilms

Our study demonstrates the role of near bed flow varying at the scale of milliseconds to minutes in shaping multitrophic biofilms that matured in fluvial ecosystems under the interplay of spatial and temporal dynamics of environmental factors. Due to present understanding, effects of near bed flow change in accordance to the successional stage of biofilms with clear effects on intermediate and negligible effects on later successional stages (Horner and Welch 1981; Besemer et al. 2007). Our study focused on biofilms that developed in the fluvial environment, rather than on biofilms of a distinct successional stage grown on artificial surfaces. We demonstrated clear seasonal variations of the fluvial biofilm community structure. Despite these seasonal differences, our field study showed both within and across guild responses of fluvial biofilms toward near bed flow with consequences for both diversity and trophic structure.

Risse-Buhl et al. (2017) were the first to demonstrate the importance of near bed turbulence (i.e., TKE) in shaping the composition and spatial architecture of fluvial biofilms. Here, we analyzed microbial communities based on morphotypes and rRNA-fingerprinting profiles and used a more detailed characterization of the microscale near bed flow by quantifying both TKE and $\bar{u}$. The actual values of TKE and $\bar{u}$ are expected to depend on measurement height and size of the sampling volume of the ADV. Turbulent velocity fluctuations and the resulting bed shear stress are governed by spectral energy transfer from large to small scales (energy cascade). Although the smallest turbulent eddies, which are affected by viscosity of water, were not fully resolved in our study, their kinetic energy can be expected to scale with observed TKE of the energy-containing scales (Biggs et al. 2005). We are aware that instantaneous flow field observations are a "snap shot" whereas biofilms have developed over longer time scales resulting in a mismatch of temporal scales. This mismatch can be considered as one cause for the relatively large scatter. Fluvial biofilms had at least 3 weeks for their development following a bankfull discharge event, which is considered sufficient to reach mature biofilm stages (Biggs 1996). Thus, we expect flow measurements to be representative for the time the biofilms developed and that the variability among sampling sites scale with the physical forcing relevant for the biofilm community and trophic interactions.

Both parameters TKE and $\bar{u}$ varied over one- to two-orders of magnitude spanning a niche space in which a diverse microbial community of autotrophic cyanobacteria and algae as well as heterotrophic bacteria and protists developed. Our

results clearly demonstrate that both near bed $\bar{u}$ and TKE were important physical drivers for fluvial biofilm communities. By maintaining this small-scale physical heterogeneity, more niches can be realized for a more diverse biofilm community (Besemer et al. 2009*b*), which in turn may affect the functioning of fluvial ecosystems (Singer et al. 2010; Cardinale 2011).

Local effects of flow in relation to seasonal and across-streams patterns

Even though near bed flow could explain significant variability in several community guilds for single sampling campaigns, patterns were often not consistent in space (two streams) and time (three seasons). Both the two-factorial ANCOVA and the db-RDA indicate the role of both stream and season for multitrophic communities of fluvial biofilms, which interacted with small-scale near bed flow. Variable trends of the autotroph community between streams could derive from contrasting nutrient concentrations. Above the threshold of 40 μg SRP L^{-1}, algae biomass of biofilms increase in response to flow whereas contrasting trends are observed at lower concentrations (Horner and Welch 1981; Risse-Buhl et al. 2017). Similar trends were observed in the two studied streams, where SRP concentrations were comparable to the threshold value in the nutrient richer Selke and one-order of magnitude lower in the nutrient poorer Kalte Bode.

On the temporal scale, season is known to be an important driver of changes in multitrophic community structure and microbial food web interactions of fluvial biofilms in a large river (Ackermann et al. 2011; Wey et al. 2012) and in biostabilization and biofilm erosion at increasing shear forces as a result of contrasting morphological traits of algae (Thom et al. 2015; Schmidt et al. 2016). Flow variability on larger temporal scales (i.e., flooding events), which was not the focus of this study, might have a strong effect on abundance, diversity, and trophic structure of biofilm communities besides physicochemistry (Biggs et al. 2005; Boulêtreau et al. 2006). Our data show that variations in the community structure of each microbial guild were significantly explained by seasonally differing physicochemical variables, such as temperature, light, DOC, and nutrients. Despite distinct differences in the physicochemistry of the streams, the seasonal variability was comparable at both streams. Hence, seasonal effects superimposed stream effects on guild-specific abundance and diversity, although the morphotype and T-RF pool was stream-specific. We conclude that overall biofilm dynamics was presumably driven by the seasonal differences of varying environmental boundary conditions, whereas locally the fluvial biofilms were shaped by near bed flow.

Within guild effects of flow: Abundance and diversity

Our results give evidence that near bed flow significantly affected the abundance and diversity of micro-eukaryotes, especially that of the larger sized autotrophs and heterotrophic protists, whereas that of the smaller sized bacteria was less affected. On the diversity level, we showed that the dominant bacterial members (as identified by T-RFLP) occurred irrespective of TKE, whereas the community of micro-eukaryotic T-RFs and heterotrophic protist morphotypes at high TKE was a subset of the respective community at low TKE. Former studies have shown that bacterial abundance is less reduced and is thus less susceptible to increased bed shear forces during flood disturbance or recovers faster than the abundance of larger sized taxa, for example, heterotrophic protists (Blenkinsopp and Lock 1994; Schmid-Araya 1994; Eisenmann et al. 1999; Biggs et al. 2005). Apart from the effects of large-scale flow variability such as floods, our study shows that also at baseflow conditions the abundance and diversity of microbial guilds were selected by the variability of environmental near bed flows ($\bar{u}$ and TKE).

The response of the autotroph guild and specific morphological traits toward near bed flow differed with season. At seasons where diatoms dominated the autotrophic community, their relative abundance was not affected by near bed flow. Prostrate diatom species are described to grow at high flow velocities where shear forces are high and viscous effects are negligible (Biggs et al. 1998*a*; Larned et al. 2004). Species resistant to high disturbance frequency such as *Achnanthidium* (formerly *Achnanthes*) and *Cocconeis* (e.g., Biggs et al. 1998*b*; Cardinale 2011) having a competitive advantage (Graba et al. 2014) and were observed in both TKE classes in the studied fluvial biofilms. Surprisingly, filamentous morphotypes, such as filamentous green algae and the filament forming, centric diatom *Melosira*, showed higher relative biovolumes at high TKE in the studied fluvial biofilms. Typically, filamentous morphotypes prefer areas of lower velocity since they are prone to high shear or flood disturbance (Grimm and Fisher 1989; Uehlinger 1991; Biggs and Thomsen 1995). A filamentous growth form is advantageous at lower shear where viscous effects dominate, to overcome mass transport limitation in a thin concentration boundary layer (diffusive sublayer) (Larned et al. 2004). However, filamentous taxa with specialized holdfast organelles (Tornés and Sabater 2010; Schönborn and Risse-Buhl 2013) show higher resistance to shear and also develop at high near bed flows. The filamentous autotrophs potentially reduce the physical effect of flow, that is, shear forces, on the underneath biofilms (Reiter and Carlson 1986; Blenkinsopp and Lock 1994). Furthermore, their typical undulation in the flow enhances mass transfer of nutrients toward biofilm cells (Stewart 2012; Gashti et al. 2015). Hence, filamentous autotrophs have a strong potential to promote other guilds such as heterotrophic bacteria and protists by decreasing the physical control of near bed flow. This has the potential to generate further indirect effects (i.e., mediated via morphological traits of autotrophs with direct response toward flow) of near bed flow on the multitrophic community of fluvial biofilms.

Across guild effects of flow: Trophic structure

Near bed flow affected the trophic structure of the studied fluvial biofilms especially with respect to autotrophy vs. heterotrophy as well as with respect to trophic structure. The decreasing

ratio of autotrophs to heterotrophic bacteria was driven by an increasing abundance of autotrophs and comparable bacterial abundance with increasing TKE, showing that fluvial biofilms shifted toward autotrophy. The increasing autotrophy at faster and more turbulent flows possibly leads to increased uptake of dissolved nutrients from the flowing water by the fluvial biofilms. The function of bacteria seemed to be independent from near bed flows, while they possibly shifted from utilizing DOC from the water column toward internal carbon cycling by taking up labile resources such as photosynthetic exudates of autotrophs (e.g., Risse-Buhl et al. 2012; Bengtsson et al. 2018) in more autotroph biofilms at increased near bed flow. Furthermore, the more autotroph biofilms at higher near bed flow might be a high-quality food source also for the invertebrate grazers. Our finding could provide an explanation for the larger amount of biomass removed by invertebrates when foraging in faster flows (Hintz and Wellnitz 2013).

Autotrophs potentially modulate their microenvironment by providing more spatial complexity and acting as refuge by reducing shear forces and providing additional surface for bacteria and heterotrophic protists colonizers (Lamb and Lowe 1987; Schönborn 1996*a*; Bengtsson et al. 2018). A reduction of autotrophic biomass by invertebrate grazing, dense riparian canopy cover, and frequent discharge peaks (Biggs et al. 1998*b*; Sturt et al. 2011) consequently has implications for the inhabiting microbial communities seeking refuge from increased near bed flow. Filamentous autotrophs oscillating in the flow, also known as streamers (Stoodley et al. 1999), were macroscopically visible at Kalte Bode in June 2015. These streamers are described to inhabit a specific and competitive bacterial community (Besemer et al. 2009*a*). At times of high algal biomass, bacterial diversity was not affected by near bed flow heterogeneity in flume biofilms (Besemer et al. 2009*b*). This is in line with our data showing no effect of flow but a strong positive correlation between bacteria and filamentous autotrophs. Thus, the biological control of filamentous autotrophs, that is, streamers, providing protected habitats from shear forces for the smaller sized bacteria may have offset the physical control under conditions of increased near bed flow.

The interstitial spaces of filamentous algae provide also a potential refuge for heterotrophic protists (Schönborn 1996*b*). Microcosm experiments suggest that small-sized flagellates cope with high flow by making use of microstructures, such as snail shells of *Ancylus* (Willkomm et al. 2007). This hiding response decreases their vulnerability to detachment from the surface by higher shear forces. In accordance to former studies in flumes and streams (Schmitz 1985; Primc and Habdija 1987; Risse-Buhl and Küsel 2009), we demonstrated that heterotrophic protists in fluvial biofilms are controlled by near bed flow also under complex flow conditions.

The abundance of heterotrophic protists, that is, flagellates and ciliates, decreased despite the abundance of their potential food sources, particularly bacteria and autotrophs, showed either no changes or increased with near bed flow. Although grazing by heterotrophic protists is known to shape the abundance and community structure of microbial communities (Wey et al. 2008; Weitere et al. 2018; see Fig. 3), the increasing physical force reduced their functional role at higher near bed flows. Direct observations of ciliates at fast flows revealed a higher displacement rate of motile species indicating that food uptake is inhibited (Risse-Buhl et al. 2009). On a broader scale, the bentho-pelagic coupling driven by heterotrophic protists (Weitere and Arndt 2002; Kathol et al. 2011) might be reduced since sessile ciliates remain longer in a contracted state and their uptake of suspended particles is inhibited (Risse-Buhl et al. 2009). Hence, bacteria benefitted from grazing release at conditions of increased near bed flow. Furthermore, the flow of matter from primary producers and secondary consumers toward heterotrophic protists grazers seemed to be reduced with increasing near bed flow.

Conclusions

Flow near the stream bed is an important physical driver in shaping multitrophic biofilms that matured under the interplay of spatial and seasonal varying physicochemical factors. Flow had pronounced effects on guild-specific morphological traits of autotrophs but not on functional traits of heterotrophic protists. Not only specific within guild responses of microbial communities were observed but rather multitrophic level effects, such as increased autotrophy, increased biological control via filamentous autotrophs serving as protected habitats for heterotrophic bacteria and reduced grazer control with increased near bed flow.

References

Ackermann, B., M. Esser, A. Scherwass, and H. Arndt. 2011. Long-term dynamics of microbial biofilm communities of the River Rhine with special references to ciliates. Int. Rev. Hydrobiol. **96**: 1–19. doi:10.1002/iroh.201011286

Amann, R. I., B. J. Binder, R. J. Olson, S. W. Chisholm, R. Devereux, and D. A. Stahl. 1990. Combination of 16S rRNA-targeted oligonucleotide probes with flowcytometry for analyzing mixed microbial populations. Appl. Environ. Microbiol. **56**: 1919–1925.

Augspurger, C., G. Gleixner, C. Kramer, and K. Küsel. 2008. Tracking carbon flow in a 2-week-old and 6-week-old stream biofilm food web. Limnol. Oceanogr. **53**: 642–650. doi:10.4319/lo.2008.53.2.0642

Battin, J. T., L. A. Kaplan, J. D. Newbold, and C. M. E. Hansen. 2003*a*. Contributions of microbial biofilms to ecosystem processes in stream mesocosms. Nature **426**: 439–442. doi:10.1038/nature02152

Battin, J. T., L. A. Kaplan, J. D. Newbold, C. Xianhao, and C. Hansen. 2003*b*. Effects of current velocity on the nascent architecture of stream microbial biofilms. Appl. Environ.

Microbiol. **69**: 5443–5452. doi:10.1128/AEM.69.9.5443–5452.2003

Battin, T. J., and others. 2007. Microbial landscapes: New paths to biofilm research. Nat. Rev. Microbiol. **5**: 76–81. doi:10.1038/nrmicro1556

Battin, T. J., K. Besemer, M. M. Bengtsson, A. M. Romani, and A. I. Packmann. 2016. The ecology and biogeochemistry of stream biofilms. Nat. Rev. Microbiol. **14**: 251–263. doi:10.1038/nrmicro.2016.15

Bengtsson, M. M., K. Wagner, C. Schwab, T. Urich, and T. J. Battin. 2018. Light availability impacts structure and function of phototrophic stream biofilms across domains and trophic levels. Mol. Ecol. **27**: 2913–2925. doi:10.1111/mec.14696

Berninger, U.-G., B. J. Finlay, and P. Knuppo-Leinikki. 1991. Protozoan control of bacterial abundances in freshwater. Limnol. Oceanogr. **36**: 139–147.

Besemer, K., and others. 2007. Biophysical controls on community succession in stream biofilms. Appl. Environ. Microbiol. **73**: 4966–4974. doi:10.1128/AEM.00588-07

Besemer, K., I. Hödl, G. Singer, and T. J. Battin. 2009*a*. Architectural differentiation reflects bacterial community structure in stream biofilms. ISME J. **3**: 1318–1324. doi:10.1038/ismej.2009.73

Besemer, K., G. Singer, I. Hödl, and T. J. Battin. 2009*b*. Bacterial community composition of stream biofilms in spatially variable-flow environments. Appl. Environ. Microbiol. **75**: 7189–7195. doi:10.1128/AEM.01284-09

Biggs, B. J. F. 1996. Patterns in benthic algae of streams, p. 31–56. *In* R. J. Stevenson, M. L. Bothwell, and R. L. Lowe [eds.], Algal ecology. Freshwater benthic ecosystems. Academic Press.

Biggs, B. J. F., and H. A. Thomsen. 1995. Disturbance of stream periphyton by perturbations in shear stress: Time to structural failure and differences in community resistance. J. Phycol. **31**: 233–241. doi:10.1111/j.0022-3646.1995.00233.x

Biggs, B. J. F., D. G. Goring, and V. I. Nikora. 1998*a*. Subsidy and stress responses of stream periphyton to gradients in water velocity as a function of community growth form. J. Phycol. **34**: 598–607. doi:10.1046/j.1529-8817.1998.340598.x

Biggs, B. J. F., R. J. Stevenson, and R. L. Lowe. 1998*b*. A habitat matrix conceptual model for stream periphyton. Arch. Hydrobiol. **143**: 21–56. doi:10.1127/archiv-hydrobiol/143/1998/21

Biggs, B. J. F., V. I. Nikora, and T. H. Snelder. 2005. Linking scales of flow variability to lotic ecosystem structure and function. River Res. Appl. **21**: 283–298. doi:10.1002/rra.847

Blenkinsopp, S. A., and M. A. Lock. 1994. The impact of storm-flow on river biofilm architecture. J. Phycol. **30**: 807–818. doi:10.1111/j.0022-3646.1994.00807.x

Boulêtreau, S., F. Garabétian, S. Sauvage, and J. M. Sánchez-Pérez. 2006. Assessing the importance of a self-generated detachment process in river biofilm models. Freshw. Biol. **51**: 901–912. doi:10.1002/iroh.200911203

Bryant, L. D., D. F. McGinnis, C. Lorrai, A. Brand, J. C. Little, and A. Wüest. 2010. Evaluating oxygen fluxes using micro-profiles from both sides of the sediment-water interface. Limnol. Oceanogr.: Methods **8**: 610–627. doi:10.4319/lom.2010.8.0610

Cardinale, B. J. 2011. Biodiversity improves water quality through niche partitioning. Nature **472**: 86–89. doi:10.1038/nature09904

Cox, E. J. 1997. The identification of freshwater diatoms from live material. Chapman & Hall.

De Caceres, M., and P. Legendre. 2009. Associations between species and groups of sites: Indices and statistical inference. Ecology **90**: 3566–3574. doi:10.1890/08-1823.1

Eisenmann, H., P. Burgherr, and E. I. Meyer. 1999. Spatial and temporal heterogeneity of an epilithic streambed community in relation to the habitat templet. Can. J. Fish. Aquat. Sci. **56**: 1452–1460. doi:10.1139/f99-092

Euringer, K., and T. Lueders. 2008. An optimised PCR/T-RFLP fingerprinting approach for the investigation of protistan communities in groundwater environments. J. Microbiol. Methods **75**: 262–268. doi:10.1016/j.mimet.2008.06.012

Foissner, W., and H. Berger. 1996. A user friendly guide to the ciliates (Protozoa, Ciliophora) commonly used by hydrobiologists as bioindicators in rivers, lakes, and waste waters, with notes on their ecology. Freshw. Biol. **35**: 375–482. doi:10.1016/j.mimet.2008.06.012

Gashti, M. P., J. Bellavance, O. Kroukamp, G. Wolfaardt, S. M. Taghavi, and J. Greener. 2015. Live-streaming: Time-lapse video evidence of novel streamer formation mechanism and varying viscosity. Biomicrofluidics **9**: 041101. doi:10.1063/1.4928296

Glaser, K., A. Kuppardt, S. Krohn, A. Heidtmann, H. Harms, and A. Chatzinotas. 2014. Primer pairs for the specific environmental detection and T-RFLP analysis of the ubiquitous flagellate taxa Chrysophyceae and Kinetoplastea. J. Microbiol. Methods **100**: 8–16. doi:10.1016/j.mimet.2014.02.006

Glaser, K., A. Kuppardt, J. Boenigk, H. Harms, I. Fetzer, and A. Chatzinotas. 2015. The influence of environmental factors on protistan microorganisms in grassland soils along a land-use gradient. Sci. Total Environ. **537**: 33–42. doi:10.1016/j.scitotenv.2015.07.158

Graba, M., S. Sauvage, F. Y. Moulin, G. Urrea, S. Sabater, and J. M. Sanchez-Perez. 2013. Interaction between local hydrodynamics and algal community in epilithic biofilm. Water Res. **47**: 2153–2163. doi:10.1016/j.watres.2013.01.011

Graba, M., and others. 2014. Modelling epilithic biofilms combining hydrodynamics, invertebrate grazing and algal traits. Freshw. Biol. **59**: 1213–1228. doi:10.1111/fwb.12341

Grimm, N. B., and S. G. Fisher. 1989. Stability of periphyton and macroinvertebrates to disturbance by flash floods in a desert stream. J. North Am. Benthol. Soc. **8**: 293–307. doi:10.2307/1467493

Grossmann, L., and others. 2016. Trade-off between taxon diversity and functional diversity in European lake ecosystems. Mol. Ecol. **25**: 5876–5888. doi:10.1111/mec.13878

Haack, T. K., and G. A. McFeters. 1982. Nutritional relationships among microorganisms in an epilithic biofilm community. Microb. Ecol. **8**: 115–126. doi:10.1007/BF02010445

Hart, D. D., and C. M. Finelly. 1999. Physical-biological coupling in streams: The pervasive effects of flow on benthic organisms. Annu. Rev. Ecol. Syst. **30**: 363–395. doi:10.1146/annurev.ecolsys.30.1.363

Hill, M. O. 1973. Diversity and evenness: A unifying notation and its consequences. Ecology **54**: 427–432. doi:10.2307/1934352

Hillebrand, H., C. D. Durselen, D. Kirschtel, U. Pollingher, and T. Zohary. 1999. Biovolume calculation for pelagic and benthic microalgae. J. Phycol. **35**: 403–424. doi:10.1046/j.1529-8817.1999.3520403.x

Hintz, W. D., and T. Wellnitz. 2013. Current velocity influences the facilitation and removal of algae by stream grazers. Aquat. Ecol. **47**: 235–244. doi:10.1007/s10452-013-9438-z

Horner, R. R., and E. B. Welch. 1981. Stream periphyton development in relation to current velocity and nutrients. Can. J. Fish. Aquat. Sci. **38**: 449–457. doi:10.1139/f81-062

Jeuck, A., and H. Arndt. 2013. A short guide to common heterotrophic flagellates of freshwater habitats based on the morphology of living organisms. Protist **164**: 842–860. doi:10.1016/j.protis.2013.08.003

Kamjunke, N., P. Herzsprung, and T. Neu. 2015*a*. Quality of dissolved organic matter affects planktonic but not biofilm bacterial production in streams. Sci. Total Environ. **506**: 353–360. doi:10.1016/j.scitotenv.2014.11.043

Kamjunke, N., M. Mages, O. Buttner, H. Marcus, and M. Weitere. 2015*b*. Relationship between the elemental composition of stream biofilms and water chemistry—a catchment approach. Environ. Monit. Assess. **187**: 432. doi:10.1007/s10661-015-4664-6

Kathol, M., H. Fischer, and M. Weitere. 2011. Contribution of biofilm-dwelling consumers to pelagic-benthic coupling in a large river. Freshw. Biol. **56**: 1160–1172. doi:10.1111/j.1365-2427.2010.02561.x

Koca, K., C. Noss, C. Anlanger, A. Brand, and A. Lorke. 2017. Performance of the Vectrino Profiler at the sediment–water interface. J. Hydraul. Res. **55**: 573–581. doi:10.1080/00221686.2016.1275049

Kuppardt, A., T. Fester, C. Hartig, and A. Chatzinotas. 2018. Rhizosphere protists change metabolite profiles in *Zea mays*. Front. Microbiol. **9**: 857. doi:10.3389/fmicb.2018.00857

Lamb, M. A., and R. L. Lowe. 1987. Effects of current velocity on the physical structuring of diatom (Bacillariophyceae) communities. Ohio J. Sci. **87**: 72–78.

Lane, D. J. 1991. 16S/23S rRNA sequencing, p. 115–175. *In* E. Stackebrandt and M. Goodfellow [eds.], Nucleic acid techniques in bacterial systematics. John Wiley and Sons.

Lane, D. J., B. Pace, G. J. Olsen, D. A. Stahl, M. L. Sogin, and N. R. Pace. 1985. Rapid-determination of 16S ribosomal-RNA sequences for phylogenetic analyses. Proc. Natl. Acad. Sci. USA **82**: 6955–6959. doi:10.1073/pnas.82.20.6955

Larned, S. T., V. I. Nikora, and B. J. F. Biggs. 2004. Mass-transfer-limited nitrogen and phosphorus uptake by stream periphyton: A conceptual model and experimental evidence. Limnol. Oceanogr. **49**: 1992–2000. doi:10.4319/lo.2004.49.6.1992

Li, Y., and others. 2018. Modeling the effects of hydrodynamic regimes on microbial communities within fluvial biofilms: Combining deterministic and stochastic processes. Environ. Sci. Technol. **49**: 12869–12878. doi:10.1021/acs.est.5b03277

Lock, M. A., R. R. Wallace, J. W. Costerton, R. M. Ventullo, and S. E. Charlton. 1984. River epilithon: Toward a structural-functional model. Oikos **42**: 10–22. doi:10.2307/3544604

Lorke, A., B. Müller, M. Maerki, and A. Wüest. 2003. Breathing sediments: The control of diffusive transport across the sediment-water interface by periodic boundary-layer turbulence. Limnol. Oceanogr. **48**: 2077–2085. doi:10.4319/lo.2003.48.6.2077

Majdi, N., M. Tackx, and E. Buffan-Dubau. 2012. Trophic positioning and microphytobenthic carbon uptake of biofilm-dwelling meiofauna in a temperate river. Freshw. Biol. **57**: 1180–1190. doi:10.1111/j.1365-2427.2012.02784.x

McArdle, B. H., and M. J. Anderson. 2001. Fitting multivariate models to community data: A comment on distance-based redundancy analysis. Ecology **82**: 290–297. doi:10.1890/0012-9658(2001)082[0290:Fmmtcd]2.0.Co;2

Norf, H., H. Arndt, and M. Weitere. 2009. Effects of resource supplements on mature ciliate biofilms: An empirical test using a new type of flow cell. Biofouling **25**: 769–778. doi:10.1080/08927010903174581

Oksanen, J., and others. 2017. vegan: Community ecology package. R package version 2.4-5.

Page, F. C., and F. J. Siemensma. 1991. Nackte Rhizopoden und Heliozoea, p. 1–297. *In* D. Matthes [ed.], Protozoenfauna, v. **2**. Gustav Fischer Verlag.

Patterson, D. J. 2003. Free-living freshwater protozoa: A colour guide, 1st ed. ASM Press.

Polst, B. H., and others. 2018. Hydrodynamics alter the tolerance of autotrophic biofilm communities toward herbicides. Front. Microbiol. **9**: 2884. doi:10.3389/fmicb.2018.02884

Primc, B., and I. Habdija. 1987. Ciliated colonization of artificial substrates in different saprobic conditions in a running water. Acta Hydrochim. Hydrobiol. **15**: 487–494. doi:10.1002/aheh.19870150509

R Development Core Team. 2018. R: A language and environment for statistical computing. R Foundation for Statistical Computing.

Reiter, M. A., and R. E. Carlson. 1986. Current velocity in streams and the composition of benthic algal mats. Can. J. Fish. Aquat. Sci. **43**: 1156–1162. doi:10.1139/f86-144

Risse-Buhl, U., and K. Küsel. 2009. Colonization of biofilm associated ciliate morphotypes at different flow velocities. Eur. J. Protistol. **45**: 64–76. doi:10.1016/j.ejop.2008.08.001

Risse-Buhl, U., A. Scherwass, A. Schlüssel, H. Arndt, S. Kröwer, and K. Küsel. 2009. Detachment and motility of surface-associated ciliates at increased flow velocities. Aquat. Microb. Ecol. **55**: 209–218. doi:10.3354/ame01302

Risse-Buhl, U., N. M. Trefzger, A.-G. Seifert, W. Schönborn, G. Gleixner, and K. Küsel. 2012. Tracking the authochthonous carbon flow in stream biofilm food webs. FEMS Microbiol. Ecol. **79**: 118–131. doi:10.1111/j.1574-6941.2011.01202.x

Risse-Buhl, U., and others. 2017. The role of hydrodynamics in shaping the composition and architecture of epilithic biofilms in fluvial ecosystems. Water Res. **127**: 211–222. doi:10.1016/j.watres.2017.09.054

Ritz, S., M. Eßer, H. Arndt, and M. Weitere. 2017. Large-scale patterns of biofilm-dwelling ciliate communities in a river network: Only small effects of stream order. Int. Rev. Hydrobiol. **102**: 114–124. doi:10.1002/iroh.201601880

Romaní, A. M., C. M. Borrego, V. Diaz-Villanueva, A. Freixa, F. Gich, and I. Ylla. 2014. Shifts in microbial community structure and function in light- and dark-grown biofilms driven by warming. Environ. Microbiol. **16**: 2550–2567. doi:10.1111/1462-2920.12428

Santillan, E., H. Seshan, F. Constancias, D. I. Drautz-Moses, and S. Wuertz. 2019. Frequency of disturbance alters diversity, function, and underlying assembly mechanisms of complex bacterial communities. NPJ Biofilms Microbiolomes **5**: 8. doi:10.1038/s41522-019-0079-4

Schindelin, J., and others. 2012. Fiji: An open-source platform for biological-image analysis. Nat. Methods **9**: 676–682. doi:10.1038/nmeth.2019

Schmid-Araya, J. M. 1994. Temporal and spatial distribution of benthic microfauna in sediments of a gravel streambed. Limnol. Oceanogr. **39**: 1813–1821. doi:10.4319/lo.1994.39.8.1813

Schmidt, H., M. Thom, L. King, S. Wieprecht, and S. U. Gerbersdorf. 2016. The effect of seasonality upon the development of lotic biofilms and microbial biostabilisation. Freshw. Biol. **61**: 963–978. doi:10.1111/fwb.12760

Schmitz, M. 1985. Ökologische und systematische Untersuchungen an Ciliaten (Protozoa, Ciliophora) des Rheines bei Bonn, BRD. Proc. Int. Assoc. Theor. Appl. Limnol. **22**: 2292–2296.

Schönborn, W. 1996*a*. Algal aufwuchs on stones, with particular reference to the *Cladophora* - dynamics in a small stream (Ilm, Thuringia, Germany): Production, decomposition and ecosystem reorganizer. Limnologica **26**: 375–383.

Schönborn, W. 1996*b*. Colonization and structure of natural and artificial microhabitats (stone and slide surfaces, interstitial spaces between algal and wool filaments, as well as in sediments and foamed plastic) in the Ilm, a small stream of the middle mountain region (Thuringia, Germany). Limnologica **26**: 385–391.

Schönborn, W., and U. Risse-Buhl. 2013. Lehrbuch der Limnologie, 2nd ed. Schweizerbart'sche Verlagsbuchhandlung.

Singer, G., K. Besemer, P. Schmitt-Kopplin, I. Hödl, and T. J. Battin. 2010. Physical heterogeneity increases biofilm resource use and its molecular diversity in stream mesocosms. PLoS One **5**: e9988. doi:10.1371/journal.pone.0009988

Smirnov, A. V., and A. V. Goodkov. 1999. An illustrated list of basic morphotypes of Gymnamoebia (Rhizopoda, Lobosea). Protist **1**: 20–29.

Statzner, B., J. A. Gore, and V. H. Resh. 1988. Hydraulic stream ecology: Observed patterns and potential applications. J. North Am. Benthol. Soc. **7**: 307–360. doi:10.2307/1467296

Stevenson, R. J. 1996. The stimulation and drag of current, p. 321–340. *In* R. J. Stevenson, M. L. Bothwell, and R. L. Lowe [eds.], Algal ecology: Freshwater benthic ecosystems. Academic Press.

Stewart, P. S. 2012. Mini-review: Convection around biofilms. Biofouling **28**: 187–198. doi:10.1080/08927014.2012.662641

Stoodley, P., I. Dodds, J. D. Boyle, and H. M. Lappin-Scott. 1999. Influence of hydrodynamics and nutrients on biofilm structure. J. Appl. Microbiol. **85**: 19S–28S. doi:10.1111/j.1365-2672.1998.tb05279.x

Sturt, M. M., M. A. K. Jansen, and S. S. C. Harrison. 2011. Invertebrate grazing and riparian shade as controllers of nuisance algae in a eutrophic river. Freshw. Biol. **56**: 2580–2593. doi:10.1111/j.1365-2427.2011.02684.x

Teodósio, J., M. Simões, L. Melo, and F. Mergulhão. 2010. Flow cell hydrodynamics and their effects on *E. coli* biofilm formation under different nutrient conditions and turbulent flow. Biofouling **27**: 1–11. doi:10.1080/08927014.2010.535206

Thom, M., H. Schmidt, S. U. Gerbersdorf, and S. Wieprecht. 2015. Seasonal biostabilization and erosion behavior of fluvial biofilms under different hydrodynamic and light conditions. Int. J. Sediment Res. **30**: 273–284. doi:10.1016/j.ijsrc.2015.03.015

Tornés, E., and S. Sabater. 2010. Variable discharge alters habitat suitability for benthic algae and cyanobacteria in a forested Mediterranean stream. Mar. Freshw. Res. **61**: 441–450. doi:10.1071/MF09095

Uehlinger, U. 1991. Spatial and temporal variability of the periphyton biomass in a prealpine river (Necker, Switzerland). Arch. Hydrobiol. **123**: 219–237.

van Dorst, J., and others. 2014. Community fingerprinting in a sequencing world. FEMS Microbiol. Ecol. **89**: 316–330. doi:10.1111/1574-6941.12308

Weitere, M., and H. Arndt. 2002. Water discharge-regulated bacteria-heterotrophic nanoflagellate (HNF) interactions in the water column of the River Rhine. Microb. Ecol. **44**: 19–29. doi:10.1007/s00248-002-2010-3

Weitere, M., and others. 2018. The food web perspective on aquatic biofilms. Ecol. Monogr. **88**: 543–559. doi:10.1002/ecm.1315

Wetzel, R. G. 2001. Limnology: Lake and river ecosystems, 3rd ed. Academic Press.

Wey, J., A. Scherwass, H. Norf, H. Arndt, and M. Weitere. 2008. Effects of protozoan grazing within river biofilms under semi-natural conditions. Aquat. Microb. Ecol. **52**: 283–296. doi:10.3354/ame01236

Wey, J. K., K. Jürgens, and M. Weitere. 2012. Seasonal and successional influences on bacterial community composition exceed that of protozoan grazing in river biofilms. Appl. Environ. Microbiol. **78**: 2013–2024. doi:10.1128/Aem.06517-11

Whittaker, R. H. 1972. Evolution and measurement of species diversity. Taxon **21**: 213–251. doi:102307/1218190

Willkomm, M., A. Schlüssel, E. Reiz, and H. Arndt. 2007. Effects of microcurrents in the boundary layer on the attachment of benthic heterotrophic nanoflagellates. Aquat. Microb. Ecol. **48**: 169–174. doi:10.3354/ame048169

Wollschläger, U., and others. 2017. The Bode hydrological observatory: A platform for integrated, interdisciplinary hydro-ecological research within the TERENO Harz/Central German Lowland Observatory. Environ. Earth Sci. **76**:29. doi:10.1007/s12665-016-6327-5

Acknowledgments

We appreciate the support by Peter Portius and his team for technical support, Clara Mendoza-Lera, Nicole Oberhoffner, Martin Diener and Sven Bauth for field assistance, Ute Link for carrying out the microscopic quantification of bacteria and autotrophs, and Verena Jaschik for technical support of T-RFLP analysis. The research profited from the TERENO (Terrestrial Environmental Observatories) infrastructure. We acknowledge the helpful comments of the two anonymous reviewers. The project was financed by research grants from the German Research Foundation (WE 3545/6-1, LO 1150/8-1, and RI 2093/2-1).

Conflict of Interest

None declared.

Submitted 17 September 2019
Revised 23 January 2020
Accepted 09 March 2020

Associate editor: Anna Romaní